



SPE 89874

Generalized Capillary Pressure and Relative Permeability Model Inferred from Fractal Characterization of Porous Media

Kewen Li, SPE, Stanford University

Copyright 2004, Society of Petroleum Engineers Inc.

This paper was prepared for presentation at the SPE Annual Technical Conference and Exhibition held in Houston, Texas, U.S.A., 26–29 September 2004.

This paper was selected for presentation by an SPE Program Committee following review of information contained in a proposal submitted by the author(s). Contents of the paper, as presented, have not been reviewed by the Society of Petroleum Engineers and are subject to correction by the author(s). The material, as presented, does not necessarily reflect any position of the Society of Petroleum Engineers, its officers, or members. Papers presented at SPE meetings are subject to publication review by Editorial Committees of the Society of Petroleum Engineers. Electronic reproduction, distribution, or storage of any part of this paper for commercial purposes without the written consent of the Society of Petroleum Engineers is prohibited. Permission to reproduce in print is restricted to a proposal of not more than 300 words; illustrations may not be copied. The proposal must contain conspicuous acknowledgment of where and by whom the paper was presented. Write Librarian, SPE, P.O. Box 833836, Richardson, TX 75083-3836, U.S.A., fax 01-972-952-9435.

Abstract

The Brooks-Corey capillary pressure model has been accepted widely in the petroleum and other industries. However the Brooks-Corey model cannot represent capillary pressure curves of some rock samples such as those from The Geysers geothermal field. In fact, few existing capillary pressure models work for these rock samples. To this end, a more general capillary pressure model was derived theoretically from fractal modeling of a porous medium. It was found that the more general capillary pressure model could be reduced to the frequently-used Brooks-Corey capillary pressure model and the Li-Horne imbibition model when the fractal dimension of a porous medium takes a limiting value. This also demonstrates that the Brooks-Corey model and the Li-Horne model, which have been proposed empirically, have a solid theoretical basis. The results demonstrated that the new capillary pressure model could represent the capillary pressure curves of The Geysers rock while the Brooks-Corey model cannot. A relative permeability model was also developed from the new capillary pressure model. Fractal dimension, a parameter associated with the heterogeneity of the rock, determines the shape of relative permeability curves according to the new relative permeability model. The model can also be reduced to the Brooks-Corey relative permeability model.

Introduction

It is essential to represent capillary pressure and relative permeability curves mathematically in an appropriate way because both are important parameters in reservoir engineering. There have been a number of existing capillary pressure¹⁻¹¹ and relative permeability models¹²⁻¹⁴. Many engineering decisions regarding the development of oil and gas fields are made based on predictions using these models. Engineering and financial risks may be reduced if the capillary

pressure and relative permeability models can characterize the multiphase fluid flow in reservoirs accurately.

In 1954, Corey¹ found that oil-gas capillary pressure curves could be expressed approximately using the following linear relation:

$$1/P_c^2 = CS_w^* \quad (1)$$

where P_c is the capillary pressure, C is a constant, and S_w^* is the normalized wetting phase saturation, which could be expressed as follows in the drainage case:

$$S_w^* = \frac{S_w - S_{wr}}{1 - S_{nwi} - S_{wr}} \quad (2)$$

where S_{nwi} is the initial saturation of the nonwetting phase and S_{wr} is the residual saturation of the wetting phase. In Corey's case, S_{wr} was the residual oil saturation and S_{nwi} was equal to zero.

In 1960, Thomeer² proposed a relationship between capillary pressure and mercury saturation empirically:

$$P_c = p_e \left(\frac{S_{Hg}}{S_{Hg\infty}} \right)^{\frac{1}{F_g}} \quad (3)$$

where p_e is the entry capillary pressure of the rock sample, S_{Hg} is the mercury saturation, $S_{Hg\infty}$ is the mercury saturation at an infinite capillary pressure, and F_g is the pore geometrical factor.

In 1966, Brooks and Corey³ modified the capillary pressure function to a more general form as follows:

$$P_c = p_e (S_w^*)^{-1/\lambda} \quad (4)$$

where λ is the pore size distribution index. Note that the wetting phase is air and the nonwetting phase is mercury in the case of an air-mercury fluid pair.

The Brooks-Corey³ model is similar to the Thomeer² model. The difference between the two is the definition of the normalized saturation.

In 1980, Van Genuchten⁴ adopted a capillary pressure model to predict the hydraulic conductivity of unsaturated soils. The model is expressed as follows:

$$S_w^* = [1 + (aP_c)^n]^{-c} \quad (5)$$

where a , c , and n are parameters to be determined. Note that S_{nwi} was equal to zero in the case of Van Genuchten⁴.

In 1998, Jing and Van Wunnik⁵ proposed a capillary pressure function to interpret the data of core-scale flow experiments. The function is expressed as follows:

$$P_c = p_c^0 \left[\left(\frac{d}{S_w - S_{wr}} \right)^n + a \right] \quad (6)$$

where p_c^0 is the capillary pressure scaling factor, d is a constant to define the curvature, n is the asymmetry shape factor, and a is a constant to control the value of the entry capillary pressure.

Among all the capillary pressure models described previously, the Brooks-Corey capillary pressure model³ has been used frequently for the consolidated porous media. In the case of unconsolidated porous media, the most frequently used capillary pressure model is the Van Genuchten⁴ model.

Empirically it has been found that the Brooks-Corey capillary pressure model is appropriate to the drainage case. To this end, Li and Horne⁶ proposed a capillary pressure model for the imbibition case in 2001. The model is expressed as follows:

$$P_c = p_{\max} (1 - S_w^*)^{-\frac{1}{\lambda}} \quad (7)$$

where p_{\max} is the capillary pressure at the residual nonwetting phase saturation.

In 1995, Skelt and Harrison⁷ proposed an empirical model to describe the relationship between water saturation and reservoir height above the oil-water contact. The model is expressed as follows:

$$S_w = 1 - a \exp\left(\frac{-b_0}{P_c + d}\right)^c \quad (8)$$

where a , b_0 , c , and d are constants. Note that P_c is equal to the reservoir height above the oil-water contact in this case.

There have been other capillary pressure models under different conditions such as those proposed by Huang *et al.*⁸ and Lenormand⁹.

One common feature of the capillary pressure models described previously is that all were proposed empirically. The parameters (for example, a , b_0 , c , and d in Eq. 8) involved in these models do not have a physical significance. Recently Li¹⁵ derived the empirical Brooks-Corey capillary pressure model theoretically from fractal modeling of a porous

medium. The theoretical development shows that the Brooks-Corey capillary pressure model, once considered as empirical, has a solid theoretical basis. This may also explain why the Brooks-Corey capillary pressure model works so well in many cases. However there have still been experimental data for which the Brooks-Corey capillary pressure model³ does not work.

Li and Horne¹⁶ reported that the Brooks-Corey capillary pressure model could be used to represent the curves of the rock without fractures (for example, Berea sandstone) but not for rock samples with many fractures (for example, the rock from The Geysers geothermal field).

In a previous paper¹⁷, the author also reported that the Brooks-Corey capillary pressure model³ could work for some rock samples but not for others, even from the same reservoir.

Interestingly, Li and Horne¹⁶ found that fractal curves inferred from capillary pressure data were good straight lines for all the rock samples, both those with and those without fractures. The fractal curves represent the relationship between the number of pores and the radius of the pore throats. Later the author¹⁷ found similar phenomena for the core samples from an oil reservoir.

This finding implies that a more general capillary pressure model may exist to represent both the rock in which the Brooks-Corey model works and the rock in which the Brooks-Corey model does not work. In this study, such a generalized capillary pressure model was derived theoretically from fractal modeling.

Relative permeability can be calculated from capillary pressure. There have been many methods to do so as reviewed recently Li and Horne¹⁸. In this study, a new relative permeability model was developed based on the generalized capillary pressure model. Experimental data were used to test the new capillary pressure and relative permeability models.

Theory

A more general capillary pressure and relative permeability model was derived theoretically from fractal modeling. The results are presented and discussed in this section. The detail derivation of the new model is shown in Appendix A.

A more general capillary pressure model

The new capillary pressure model using a fractal modeling technique is expressed as follows:

$$P_c = p_{\max} (1 - bS_w^*)^{-\frac{1}{\lambda}} \quad (9)$$

where p_{\max} is the capillary pressure at the residual nonwetting phase saturation in the imbibition case and the capillary pressure at the residual wetting phase saturation in the drainage case. b is a constant and expressed as follows:

$$b = 1 - \left(\frac{P_e}{p_{\max}} \right)^{-\lambda} \quad (10)$$

where $\lambda = 3 - D_f$. D_f is the fractal dimension, which is a representation of the heterogeneity of rock. The greater the fractal dimension, the greater the heterogeneity. Note that the pore size distribution index λ in the Brooks-Corey capillary pressure model is also a representation of the heterogeneity. The greater the pore size distribution index, the less the heterogeneity of a porous medium.

For $D_f < 3$, if p_{max} approaches infinity, then Eq. 9 can be reduced to:

$$P_c = p_e (S_w^*)^{-\frac{1}{\lambda}} \quad (11)$$

Eq. 11 is the frequently used Brooks-Corey model, which was proposed empirically by Brooks and Corey³ in 1966.

According to the derivation in Appendix A, one can see that the Brooks-Corey capillary pressure model has a solid theoretical basis. This may be why the Brooks-Corey model can be a good fit to capillary pressure curves of many real rock samples.

In the case in which $b=1$, Eq. 9 can be reduced to:

$$P_c = p_{max} (1 - S_w^*)^{-\frac{1}{\lambda}} \quad (12)$$

Eq. 12 is the imbibition capillary pressure model proposed empirically by Li and Horne⁶ in 2001.

In the case in which $b=0$, Eq. 9 can be reduced to:

$$P_c = p_{max} \quad (13)$$

Eq. 13 may be considered a capillary pressure model for a single capillary tube.

One can see that Eq. 9, as a generalized capillary pressure model, could be applied in both a complicated porous medium and in a single capillary tube as well as in both drainage and imbibition cases.

Differentiating Eq. 9, one can obtain the following relationship:

$$\frac{dS_w^*}{dP_c} \propto -P_c^{-(4-D_f)} \quad (14)$$

Eq. 14 can also be expressed as:

$$\frac{dS_{Hg}}{dP_c} \propto P_c^{-(4-D_f)} \quad (15)$$

Eq. 15 was also derived by Friesen and Mikula¹⁹ in 1987 using a different method.

A new relative permeability model

The relative permeability models inferred from the generalized capillary pressure model are presented and discussed in this section. As pointed out by Li and Horne¹⁸, the Purcell relative permeability model may be the best fit to the wetting phase relative permeability and the Brooks-Corey relative permeability model may be used to calculate the nonwetting phase relative permeability once reliable capillary pressure data are available. Therefore relative permeability models were derived using the Purcell and the Brooks-Corey approaches respectively.

Based on the Purcell approach

The new relative permeability model derived from the generalized capillary pressure model using the Purcell approach is expressed as follows:

$$k_{rw} = \frac{1 - (S_{we})^{\frac{2+\lambda}{\lambda}}}{1 - \alpha^{\frac{2+\lambda}{\lambda}}}, \text{ (wetting phase)} \quad (16)$$

$$k_{rmw} = \frac{(S_{we})^{\frac{2+\lambda}{\lambda}} - \alpha^{\frac{2+\lambda}{\lambda}}}{1 - \alpha^{\frac{2+\lambda}{\lambda}}}, \text{ (nonwetting phase)} \quad (17)$$

where k_{rw} and k_{rmw} are the relative permeability of the wetting phase and the nonwetting phase, S_{we} is defined as follows:

$$S_{we} = 1 - bS_w^* \quad (18)$$

and α is defined as follows:

$$\alpha = \left(\frac{P_e}{P_{max}}\right)^{-\lambda} \quad (19)$$

According to Eq. 16:

$$k_{rw}(S_w^* = 0) = 0 \quad (20)$$

and

$$k_{rw}(S_w^* = 1) = 1 \quad (21)$$

According to Eq. 17:

$$k_{rmw}(S_w^* = 0) = 1 \quad (22)$$

and

$$k_{rmw}(S_w^* = 1) = 0 \quad (23)$$

The previous results of end-point relative permeability for both wetting phase and nonwetting phase show, to some extent, the validity of the new relative permeability model.

One can see from Eqs. 16 and 17 that relative permeability depends not only upon the heterogeneity (represented by fractal dimension through the parameter λ) but also upon the pore size of porous media, represented by the entry capillary pressure and the maximum capillary pressure, in some cases.

When $D_f < 3$ and p_{max} approaches infinity, Eqs. 16 and 17 can also be reduced to the simple Purcell relative permeability model expressed as follows:

$$k_{rw} = (S_w^*)^{\frac{2+\lambda}{\lambda}} \quad (24)$$

$$k_{rmw} = 1 - (S_w^*)^{\frac{2+\lambda}{\lambda}} \quad (25)$$

Therefore the new relative permeability model (Eqs. 16 and 17) encompasses the Purcell relative permeability model (Eqs. 24 and 25).

In cases where p_{max} has a finite value, Eqs. 16 and 17 can be written as follows:

$$k_{rw} = \frac{1 - (1 - bS_w^*)^m}{1 - (1 - b)^m} \quad (26)$$

$$k_{rmw} = \frac{(1 - bS_w^*)^m - (1 - b)^m}{1 - (1 - b)^m} \quad (27)$$

where $b = 1 - \alpha$ and m is expressed as follows:

$$m = \frac{2 + \lambda}{\lambda} = \frac{5 - D_f}{3 - D_f} \quad (28)$$

Note that m is a parameter associated with the heterogeneity of the porous medium because the fractal dimension D_f is a representation of heterogeneity. Parameter b is associated with the pore size.

Based on the Burdine model

The new relative permeability model derived from the generalized capillary pressure model using the Burdine approach is expressed as follows:

$$k_{rw} = \frac{1 - (S_{we})^{\frac{2+\lambda}{\lambda}}}{1 - \alpha^{\frac{2+\lambda}{\lambda}}} (S_w^*)^2 \quad (29)$$

and

$$k_{rmw} = \frac{(S_{we})^{\frac{2+\lambda}{\lambda}} - \alpha^{\frac{2+\lambda}{\lambda}}}{1 - \alpha^{\frac{2+\lambda}{\lambda}}} (1 - S_w^*)^2 \quad (30)$$

When $D_f < 3$ and p_{max} approaches infinity, Eqs. 29 and 30 can be reduced to the simple Brooks-Corey relative permeability model. The model is expressed as follows:

$$k_{rw} = (S_w^*)^{\frac{2+3\lambda}{\lambda}} \quad (31)$$

$$k_{rmw} = (1 - S_w^*)^2 [1 - (S_w^*)^{\frac{2+\lambda}{\lambda}}] \quad (32)$$

Therefore the new relative permeability model (Eqs. 29 and 30) based on the Burdine approach encompasses the Brooks-Corey relative permeability model (Eqs. 31 and 32).

In the case in which p_{max} has a finite value, Eqs. 29 and 30 can be expressed as follows:

$$k_{rw} = \frac{(S_w^*)^2 [(1 - bS_w^*)^m - 1]}{(1 - b)^m - 1} \quad (33)$$

$$k_{rmw} = \frac{(1 - S_w^*)^2 [(1 - b)^m - (1 - bS_w^*)^m]}{(1 - b)^m - 1} \quad (34)$$

In the case in which $b=1$ and $m>0$, Eqs. 33 and 34 can be reduced as follows:

$$k_{rw} = (S_w^*)^2 [1 - (1 - S_w^*)^m] \quad (35)$$

$$k_{rmw} = (1 - S_w^*)^{2+m} \quad (36)$$

In the case in which $m=0$, Eqs. 35 and 36 can be reduced as follows:

$$k_{rw} = (S_w^*)^2 \quad (37)$$

$$k_{rmw} = (1 - S_w^*)^2 \quad (38)$$

However it is not clear under what circumstances m is equal to zero. Note that $m=0$ implies that $D_f=5$.

Results

The new capillary pressure and relative permeability models were tested and the results are discussed in this section.

Generalized capillary pressure model

The theoretical capillary pressure data were calculated using Eq. 9 with different values of fractal dimension and the results are shown in Fig. 1. The values of fractal dimension used in the calculation were 2.0, 2.5, 2.9, 3.3 and 3.8. The values of maximum capillary pressure and entry capillary pressure were 100 atm and 0.4 atm respectively in Fig. 1. The residual wetting-phase saturation was 20%. In the case where $D_f < 3.0$, the capillary pressure curve is convex to the axis of the wetting-phase saturation and looks like a common capillary pressure curve (for example, the capillary pressure curve of Berea sandstone). This type of capillary pressure curve can usually be represented mathematically by the Brooks-Corey model in cases in which p_e/p_{max} is negligible. In the case where $D_f > 3.0$, the capillary pressure curve is concave to the axis of the wetting-phase saturation (see Fig. 1). The capillary pressure curves of The Geysers rock have such a feature¹⁶.

Fig. 2 shows the normalized capillary pressure curves using the data shown in Fig. 1. In the case in which D_f is equal to 2.0, the relationship between capillary pressure and the normalized wetting phase saturation is linear. However the normalized capillary pressure curves with D_f other than 2.0 are not straight lines, which demonstrates that D_f influences not only the magnitude of capillary pressure but also the shape of the curves (see Fig. 2).

The effect of p_e on the shape of capillary pressure curves is shown in Fig. 3. D_f is equal to 2.5 and $p_{max}=100$ atm in Fig. 3. One can see that the relationship between capillary pressure and the normalized wetting phase saturation is linear if p_e is less than a specific value. Otherwise, it is not linear. When D_f increases from 2.5 to 2.9, the normalized capillary pressure curves calculated using Eq. 9 are plotted in Fig. 4. In this case, all the curves are highly nonlinear.

Fig. 5 shows the effect of p_{max} on the capillary pressure curves. D_f is equal to 2.5 and $p_e=0.4$ atm in Fig. 5. The value of p_{max} ranges from 10 to 10^5 atm. The normalized capillary pressure curves are linear if p_{max} is greater than a specific value. When D_f increases from 2.5 to 2.9, the normalized capillary pressure curves calculated using Eq. 9 are plotted in Fig. 6. With $D_f=2.9$, all the curves become nonlinear.

According to the results shown in Figs. 3-6, the values of p_e and p_{max} , like D_f , influence not only the value of capillary pressure but also the shape of the curves.

A typical capillary pressure curve of The Geysers rock is shown in Fig. 7. The capillary pressure curve was measured using a mercury intrusion technique. It is obvious that the Brooks-Corey model cannot represent such a curve. The new capillary pressure model (Eq. 9) developed in this study was

used to match the data and the results are demonstrated in Fig. 7. One can see that the new capillary pressure model can represent the data of The Geysers rock satisfactorily. The values of parameters obtained by the match were: $p_{max}=1.837 \times 10^3$ atm, $b=0.984$, and $D_f=3.483$.

The capillary pressure data of Berea sandstone, measured using a mercury intrusion technique, was also modeled using the new model and the results are plotted in Fig. 7. In this case, Eq. A-17, instead of Eq. 9 (reduced form of Eq. A-17), was used. This is because Eq. A-17 may not be reduced to Eq. 9 if p_{max} approached infinity. One can see that the new model can also fit the capillary pressure curve of Berea sandstone appropriately. The values of parameters obtained by the match were: $p_{max}=1.0 \times 10^4$ atm, $p_e=0.28$ atm, and $D_f=2.33$. The Brooks-Corey model can be applied directly if the normalized capillary pressure curve is linear on a log-log plot. This is because the generalized capillary pressure model (Eq. 9) can be reduced to the Brooks-Corey model in this case.

More examples verifying the new capillary pressure model (Eq. 9) were reported recently by Li and Horne in another paper²⁰. Note that the capillary pressure tube model used by Li and Horne²⁰ was different from that used in this study. Li and Horne²⁰ used a capillary pressure tube model with a radius of r and a fixed length of l instead of being equal to r . Therefore the relationship between λ and D_f used by Li and Horne²⁰ was $\lambda=2-D_f$.

New relative permeability model

The wetting phase relative permeability was calculated using Eq. 16 and the nonwetting phase relative permeability was calculated using Eq. 30 with different values of fractal dimension. The reason to do this was because Li and Horne¹⁸ reported that the Purcell model is the best fit to the experimental data of the wetting phase relative permeability for both drainage and imbibition processes but is not a good fit for the nonwetting phase. The results are plotted in Fig. 8. One can see that the relative permeability curves of the nonwetting phase are almost the same for different values of fractal dimension. However the relative permeability curves of the wetting phase are different for different values of fractal dimension. Fig. 8 shows that the wetting phase relative permeability curves with fractal dimension greater than 3.0 have different features from those with fractal dimension less than 3.0, as predicted by the model (see Eq. 16). One can see that the values of the wetting phase relative permeability in the case where the fractal dimension over 3 are very small until the wetting phase saturation reaches about 80%. This phenomenon may be verified by future experimental data of relative permeability measured in The Geysers rock.

Few experimental data of relative permeability in The Geysers rock or other type of rock with fractal dimension greater than 3.0 have been available in the literature. Therefore we cannot verify the new relative permeability models at present.

Conclusions

Based on the present study, the following conclusions may be drawn:

1. A more general model has been developed to represent capillary pressure curves of a porous medium using fractal modeling.
2. The new capillary pressure model can represent the experimental data of the very heterogeneous rock from The Geysers geothermal field satisfactorily. However the Brooks-Corey capillary pressure model cannot.
3. The theoretical derivation conducted in this study demonstrated that the Brooks-Corey model for the drainage case and the Li-Horne model for the imbibition case may have a solid theoretical basis.
4. In addition to fractal dimension, the shape of capillary pressure curves is also influenced by p_e and p_{max} in the cases where D_f is greater than 3.
5. New relative permeability models for both wetting and nonwetting phases have been developed, based on the generalized capillary pressure model.

Acknowledgments

This research was conducted with financial support from the US Department of Energy under grant DE-FG07-02ID14418, the contribution of which is gratefully acknowledged. The author would like to acknowledge Roland N. Horne for his invaluable discussion and suggestions.

Nomenclature

a	= constant
b	= constant defined in Eq. 10
b_0	= constant
C	= constant
d	= constant
D_f	= fractal dimension
F_g	= pore geometrical factor
k_{rmw}	= relative permeability of nonwetting phase
k_{rw}	= relative permeability of wetting phase
n	= constant
$N(r)$	= number of the units needed to fill a fractal object
m	= constant defined in Eq. 28
m_0	= constant
p_c^0	= capillary pressure scaling factor
P_c	= capillary pressure
p_e	= entry capillary pressure
p_{max}	= capillary pressure at residual wetting phase saturation in drainage case
r	= radius
S_e	= equilibrium saturation of the nonwetting phase
S_{Hg}	= mercury saturation
S_{Hg^∞}	= mercury saturation at an infinite capillary pressure
S_m	= minimum wetting phase saturation from the capillary pressure curve
S_{nw}	= nonwetting phase saturation
S_{nwi}	= initial saturation of the nonwetting phase
S_w	= wetting phase saturation
S_w^*	= normalized wetting-phase saturation

S_{we} = pseudo saturation defined in Eq. 18.

S_{wr} = residual saturation of the wetting phase

V_{Hg} = cumulative volume of mercury intruded into rock

V_p = pore volume

λ = pore size distribution index

λ_{rw} = tortuosity ratio of wetting phase

λ_{rmw} = tortuosity ratio of nonwetting phase

τ_{nw} = tortuosity of nonwetting phase

τ_w = tortuosity of wetting phase

θ = contact angle

σ = interfacial tension

References

1. Corey, A. T.: "The Interrelation between Gas and Oil Relative Permeabilities", *Prod. Mon.*, (1954), **19**, 38.
2. Thomeer, J.H.M.: "Introduction of a Pore Geometrical Factor Defined by the Capillary Pressure," *Trans. AIME*, (1960), **219**, 354.
3. Brooks, R. H. and Corey, A. T.: "Properties of Porous Media Affecting Fluid Flow", *J. Irrig. Drain. Div.*, (1966), **6**, 61.
4. Van Genuchten, M.Th.: "A Closed-Form Equation for Predicting the Hydraulic Conductivity of Unsaturated Soils," *Soil Sci. Soc. Am. J.* (1980), V.44, No.5, 892.
5. Jing, X.D. and Van Wunnik, J.N.M.: "A Capillary Pressure Function for Interpretation of Core-Scale Displacement Experiments," SCA 9807, Proceedings of 1998 International Symposium of the Society of Core Analysts, The Hague, Netherlands, Sept. 14-16, 1998.
6. Li, K. and Horne, R.N.: "An Experimental and Theoretical Study of Steam-Water Capillary Pressure," *SPEREE* (December 2001), p.477-482.
7. Skelt, C.H. and Harrison, B.: "An Integrated Approach to Saturation Height Analysis," Paper NNN, Proceedings of 36th SPWLA Annual Symposium, June 26-29, 1995.
8. Huang, D. D., Honarpour, M. M., Al-Hussainy, R.: "An Improved Model for Relative Permeability and Capillary Pressure Incorporating Wettability", SCA 9718, Proceedings of International Symposium of the Society of Core Analysts, Calgary, Canada, September 7-10, 1997.
9. Lenormand, R.: "Gravity-Assisted Inert Gas Injection: Micromodel Experiments and Model Based on Fractal Roughness," The European Oil and Gas Conference, Altavilla Milica, Palermo, Sicily, October 9-12, 1990.
10. Lenhard, R.J. and Oostrom, M.: "A Parametric Method for Predicting Relative Permeability-Saturation-Capillary Pressure Relationships of Oil-Water Systems in Porous Media with Mixed Wettability," *Transport in Porous Media*, V. 31, No. 1, 109, 1998.
11. Delshad, M., Lenhard, R.J., Oostrom, M., Pope, G.A., and Yang, S.: "A Mixed-Wet Hysteretic Relative Permeability and Capillary Pressure Model in a Chemical Compositional Reservoir Simulator," SPE 51891, Proceedings of the 1999 SPE Reservoir Simulation Symposium held in Houston, Texas, U.S.A., February 14-17, 2003.
12. Purcell, W.R.: "Capillary Pressures-Their Measurement Using Mercury and the Calculation of Permeability", *Trans. AIME*, (1949), **186**, 39.

13. Burdine, N. T.: "Relative Permeability Calculations from Pore Size Distribution Data," Trans. *AIME*, (1953), **198**, 71.
14. Moulou, J.-C., Vizika, O., Kalaydjian, F., and Duqueroix, J.-P.: "A New Model for Three-Phase Relative Permeabilities Based on a Fractal Representation of the Porous Media," SPE 38891, presented at the 1997 SPE Annual Technical Conference and Exhibition, San Antonio, Texas, U.S.A., 5 – 8 October 1997.
15. Li, K.: "Theoretical Development of the Brooks-Corey Capillary Pressure Model from Fractal Modeling of Porous Media," SPE 89429, Proceedings of the SPE/DOE Fourteenth Symposium on Improved Oil Recovery held in Tulsa, Oklahoma, April 17-21, 2004.
16. Li, K. and Horne, R.N.: "Fractal Characterization of the Geysers Rock," Proceedings of the GRC 2003 annual meeting, October 12-15, 2003, Morelia, Mexico; GRC Trans. V. 27 (2003).
17. Li, K.: "Characterization of Rock Heterogeneity Using Fractal Geometry," SPE 86975, Proceedings of the 2004 SPE Western Region Meeting, Bakersfield, CA, USA, March 16-18, 2004.
18. Li, K. and Horne, R.N.: "Experimental Verification of Methods to Calculate Relative Permeability Using Capillary Pressure Data," SPE 76757, Proceedings of the 2002 SPE Western Region Meeting/AAPG Pacific Section Joint Meeting held in Anchorage, Alaska, May 20-22, 2002.
19. Friesen, W.I. and Mikula, R.J.: "Fractal Dimensions of Coal Particles," *J. of Colloid and Interface Science*, V. 120, No.1, November 1987.
20. Li, K. and Horne, R.N.: "A Universal Capillary Pressure Model: Verification and Application," Proceedings of the GRC 2004 annual meeting, August 29-September 1, 2004, Palm Springs, California, USA; GRC Trans. V. 28 (2004).

Appendix A: Derivation of A Generalized Capillary Pressure and Relative Permeability Model

According to the basic concept of fractal geometry, the following expression applies to a fractal object:

$$N(r) \propto r^{-D_f} \quad (\text{A-1})$$

where r is the radius of a unit chosen to fill the fractal object, $N(r)$ is the number of the units (with a radius of r) required to fill the entire fractal object, and D_f is the fractal dimension. The fractal dimension is a representation of the heterogeneity of a fractal object. The greater the fractal dimension, the more heterogeneous the fractal object.

It has been found that most natural porous media such as reservoir rock are fractals and can be characterized using a fractal model¹⁵. The relationship between the number of pores and the radius of pores (Eq. A-1) is an example of a fractal model.

Capillary pressure curves measured by a mercury-intrusion technique are often used to infer the pore size distribution of rock samples. In making this inference, rock with a solid

skeleton and interior pores is represented by using a capillary tube model. $N(r)$ can be calculated easily once capillary pressure curves measured using a mercury-intrusion technique are available. The unit chosen in this study to represent a pore was a cylindrical capillary tube with a radius of r and a length of r . So the volume of the unit is equal to πr^3 and $N(r)$ at a given radius of r is then calculated easily.

Note that the unit chosen in previous studies¹⁵⁻¹⁷ was also a cylindrical capillary tube but the length of the tube was fixed. In this study, the length of the cylindrical capillary tube changes with the radius.

Generalized capillary pressure model

Once $N(r)$ is known, the value of fractal dimension, D_f can be determined from the relationship between $N(r)$ and r . The relationship between $N(r)$ and r should be linear on a log-log plot if the pore system of the rock is fractal.

According to the capillary tube model, $N(r)$ can be calculated as follows:

$$N(r) = \frac{V_{Hg}}{\pi r^3} \quad (\text{A-2})$$

where V_{Hg} is the cumulative volume of mercury intruded in the rock sample when capillary pressure is measured.

Combining Eq. A-1 and Eq. A-2:

$$\frac{V_{Hg}}{\pi r^3} \propto r^{-D_f} \quad (\text{A-3})$$

Arranging Eq. A-3:

$$V_{Hg} \propto r^{3-D_f} \quad (\text{A-4})$$

Considering a capillary tube model, capillary pressure can be calculated as follows:

$$P_c = \frac{2\sigma \cos \theta}{r} \quad (\text{A-5})$$

where P_c is the capillary pressure, σ is the surface tension, and θ is the contact angle.

Substituting Eq. A-5 into Eq. A-4:

$$V_{Hg} \propto P_c^{-(3-D_f)} \quad (\text{A-6})$$

The mercury saturation is calculated as follows:

$$S_{Hg} = \frac{V_{Hg}}{V_p} \quad (\text{A-7})$$

where S_{Hg} is the mercury saturation and V_p is the pore volume of the core sample.

Substituting Eq. A-7 into Eq. A-6:

$$S_{Hg} = aP_c^{-(3-D_f)} \quad (A-8)$$

here a is a constant.

When V_{Hg} increases from 0 to 0^+ , the corresponding capillary pressure increases from 0 to p_e . Eq. A-8 can be expressed as:

$$S_{Hg}(V_{Hg} \rightarrow 0) = \varepsilon = ap_e^{-(3-D_f)} \quad (A-9)$$

where ε is an infinitely small positive value close to zero and p_e is the entry capillary pressure of the rock sample.

Similarly the capillary pressure reaches a maximum value (it can also be infinite) when V_{Hg} equals a maximum value. According to Eq. A-8:

$$S_{Hg\infty} = ap_{\max}^{-(3-D_f)} \quad (A-10)$$

where $S_{Hg\infty}$ is the maximum mercury saturation and p_{\max} is the maximum capillary pressure at $S_{Hg\infty}$.

Combining Eqs. A-8, 9, and 10, one can obtain:

$$\frac{S_{Hg} - \varepsilon}{S_{Hg\infty} - \varepsilon} = \frac{P_c^{-(3-D_f)} - p_e^{-(3-D_f)}}{p_{\max}^{-(3-D_f)} - p_e^{-(3-D_f)}} \quad (A-11)$$

Considering $\varepsilon \rightarrow 0$, Eq. A-11 may be reduced to:

$$\frac{S_{Hg}}{S_{Hg\infty}} \approx \frac{P_c^{-(3-D_f)} - p_e^{-(3-D_f)}}{p_{\max}^{-(3-D_f)} - p_e^{-(3-D_f)}} \quad (A-12)$$

Using the wetting-phase saturation (the wetting-phase during mercury intrusion is air), Eq. A-12 can be expressed as:

$$\frac{1 - S_w}{1 - S_{wr}} = \frac{P_c^{-(3-D_f)} - p_e^{-(3-D_f)}}{p_{\max}^{-(3-D_f)} - p_e^{-(3-D_f)}} \quad (A-13)$$

where S_w is the wetting-phase saturation and S_{wr} is the residual saturation of the wetting-phase.

Eq. A-13 can be rearranged as:

$$\frac{1 - S_w}{1 - S_{wr}} = 1 - \frac{p_{\max}^{-(3-D_f)} - P_c^{-(3-D_f)}}{p_{\max}^{-(3-D_f)} - p_e^{-(3-D_f)}} \quad (A-14)$$

The normalized wetting-phase saturation in this case is defined as:

$$S_w^* = \frac{S_w - S_{wr}}{1 - S_{wr}} \quad (A-15)$$

Substituting Eq. A-15 into Eq. A-14:

$$S_w^* = \frac{p_{\max}^{-(3-D_f)} - P_c^{-(3-D_f)}}{p_{\max}^{-(3-D_f)} - p_e^{-(3-D_f)}} \quad (A-16)$$

Arranging Eq. A-16:

$$P_c = [p_{\max}^{-\lambda} - (p_{\max}^{-\lambda} - p_e^{-\lambda})S_w^*]^{\frac{1}{\lambda}} \quad (A-17)$$

where $\lambda = 3 - D_f$.

According to Eq. A-17, Eq. 9 in the text, the new capillary pressure model can be obtained.

A new relative permeability model

There are two main ways to infer relative permeability from capillary pressure data. One is the Purcell approach¹² and the other is the Burdine approach¹³. In this section, relative permeability models will be derived theoretically based on the new capillary pressure model (Eq. 9) using both the Purcell and the Burdine approaches.

Based on the Purcell approach

Purcell¹² developed an equation to compute permeability by using capillary pressure data. This equation can be extended readily to the calculation of multiphase relative permeability. In two-phase flow, the relative permeability of the wetting phase can be calculated as follows:

$$k_{rw} = \frac{\int_0^{S_w} dS_w / (P_c)^2}{\int_0^1 dS_w / (P_c)^2} \quad (A-18a)$$

where k_{rw} and S_w are the relative permeability and saturation of the wetting phase.

Similarly, the relative permeability of the nonwetting phase can be calculated as follows:

$$k_{rnw} = \frac{\int_{S_w}^1 dS_w / (P_c)^2}{\int_0^1 dS_w / (P_c)^2} \quad (A-18b)$$

where k_{rnw} is the relative permeability of the nonwetting phase. It can be seen from Eqs. A-18a and 18b that the sum of the wetting and nonwetting phase relative permeabilities at a specific saturation is equal to one. This may not be true in

most porous media. Comparing experimental data with the modeling data, Li and Horne¹⁸ found that the Purcell model (Eq. A-18a) may be the best fit to the experimental data of the wetting phase relative permeability for both drainage and imbibition processes but may not be a good fit for the nonwetting phase.

Substituting Eq. 9 into Eq. A-18a, one can obtain the following equation:

$$k_{rw} = \frac{\int_1^{S_{we}} (S_{we})^{\frac{2}{\lambda}} dS_{we}}{\int_1^{\alpha} (S_{we})^{\frac{2}{\lambda}} dS_{we}} \quad (\text{A-19})$$

where S_{we} and α are defined in Eq. 18 and 19 in the text respectively.

After integrating, Eq. 16 can be obtained to calculate the wetting phase relative permeability. Similarly, Eq. 17 in the text can be derived to calculate the nonwetting phase relative permeability.

Based on the Burdine model

Burdine¹³ developed equations similar to Purcell's method by introducing a tortuosity factor as a function of wetting phase saturation. The relative permeability of the wetting phase can be computed as follows:

$$k_{rw} = (\lambda_{rw})^2 \frac{\int_0^{S_w} dS_w / (P_c)^2}{\int_0^1 dS_w / (P_c)^2} \quad (\text{A-20})$$

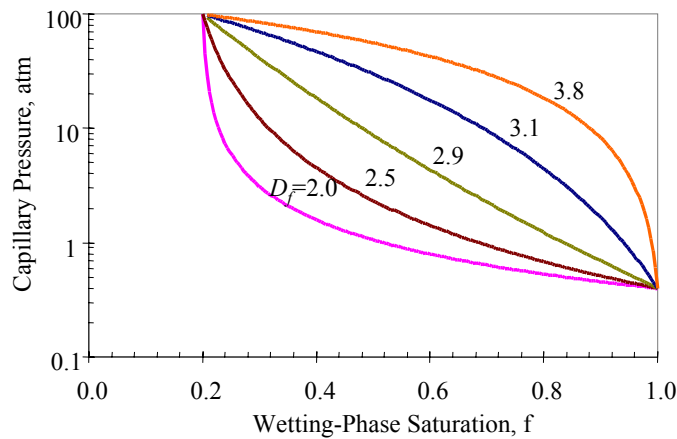


Fig. 1: Typical capillary pressure curves calculated using the new model with different values of fractal dimension.

where λ_{rw} is the tortuosity ratio of the wetting phase. According to Burdine¹³, λ_{rw} could be calculated as follows:

$$\lambda_{rw} = \frac{\tau_w(1.0)}{\tau_w(S_w)} = \frac{S_w - S_m}{1 - S_m} \quad (\text{A-21})$$

where S_m is the minimum wetting phase saturation from the capillary pressure curve; $\tau_w(1.0)$ and $\tau_w(S_w)$ are the tortuosities of the wetting phase when the wetting phase saturation is equal to 100% and S_w respectively.

In the same way, relative permeabilities of the nonwetting phase can be calculated by introducing a tortuosity ratio of the nonwetting phase. The equation can be expressed as follows:

$$k_{rnw} = (\lambda_{rnw})^2 \frac{\int_{S_w}^1 dS_w / (P_c)^2}{\int_0^1 dS_w / (P_c)^2} \quad (\text{A-22})$$

where λ_{rnw} is the tortuosity ratio of the nonwetting phase, which can be calculated as follows:

$$\lambda_{rnw} = \frac{\tau_{nw}(1.0)}{\tau_{nw}(S_w)} = \frac{1 - S_w - S_e}{1 - S_m - S_e} \quad (\text{A-23})$$

Here S_e is the equilibrium saturation of the nonwetting phase; τ_{nw} is the tortuosity of the nonwetting phase.

Using a similar procedure to that used to derive Eqs. 16 and 17, one can obtain Eqs. 29 and 30 in the text.

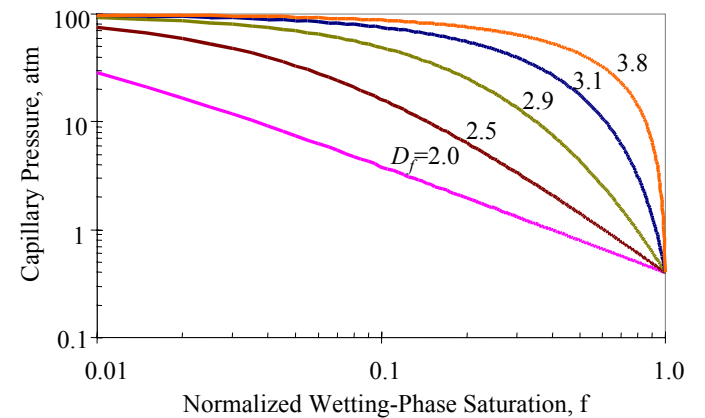


Fig. 2: Normalized capillary pressure curves calculated using the new model with different values of fractal dimension.

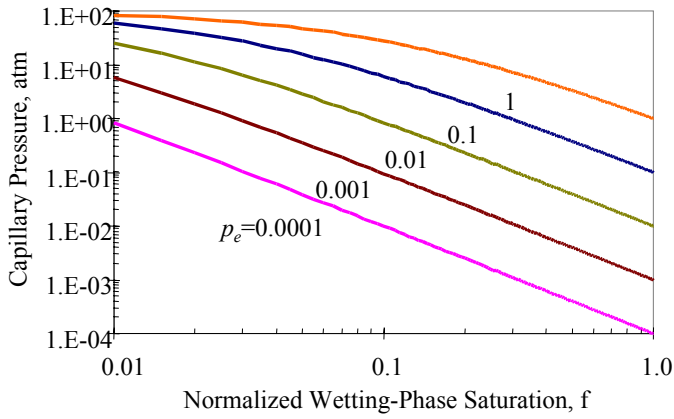


Fig. 3: Normalized capillary pressure curves calculated with different values of entry capillary pressure ($D_f=2.5$).

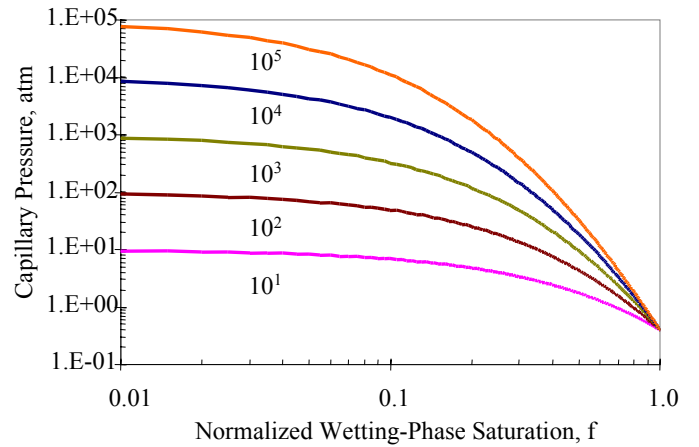


Fig. 6: Normalized capillary pressure curves calculated with different values of p_{max} ($D_f=2.9$).

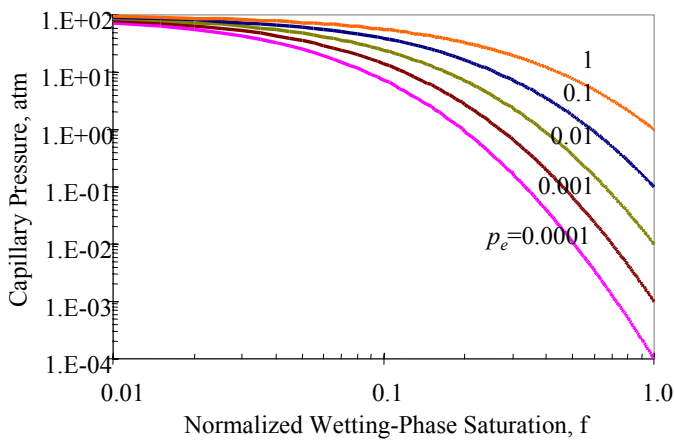


Fig. 4: Normalized capillary pressure curves calculated with different values of entry capillary pressure ($D_f=2.9$).

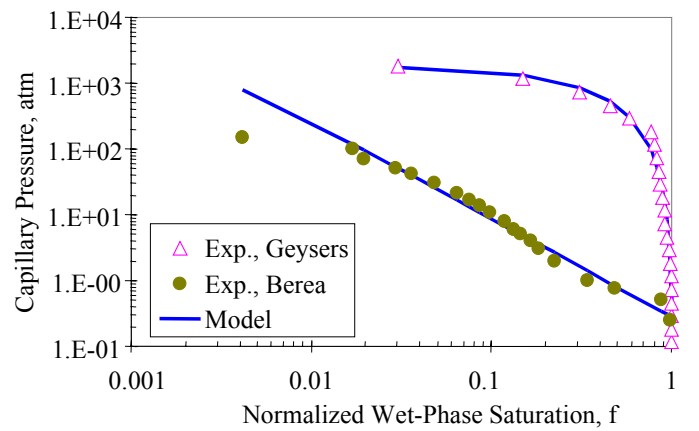


Fig. 7: Fit to the normalized capillary pressure curves of Berea sandstone and The Geysers rock.

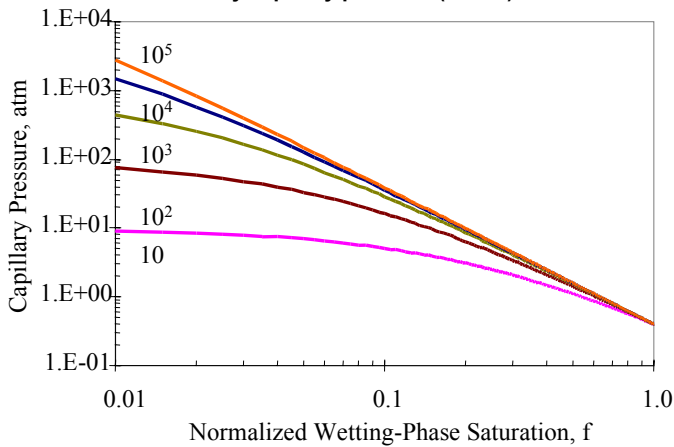


Fig. 5: Normalized capillary pressure curves calculated with different values of p_{max} ($D_f=2.5$).

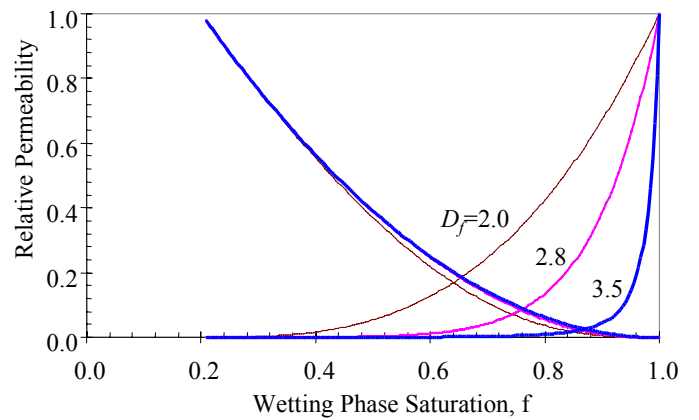


Fig. 8: Typical relative permeability curves calculated using the new model with different values of fractal dimension.